Crust Superfluidity

Implications for Macroscopic Hydrodynamics

ICONS at UvA

April 17, 2019

Vanessa Graber, McGill University

vanessa.graber@mcgill.ca

Superfluid rotation

- Superfluids can be characterised by **macroscopic wave functions** $\Psi = \Psi_0\, e^{i\varphi}$ that satisfy the Schrödinger equation. Using the standard QM formalism one can determine a **superfluid velocity**

$$\boldsymbol{v}_\mathrm{S} \equiv \frac{\boldsymbol{j}_\mathrm{S}}{\rho_\mathrm{S}} = \frac{\hbar}{m_\mathrm{c}} \nabla\varphi, \qquad \Rightarrow \qquad \boldsymbol{\omega} \equiv \nabla \times \boldsymbol{v}_\mathrm{S} = 0. \qquad (1)$$

Figure 1: Envisage vortices as tiny, rotating tornadoes. Credit: NOAA Photo Library.

- Superflow is **irrotational**: the superfluids can only rotate by forming a **regular vortex array**.

- Each vortex carries a **quantum of circulation** $\kappa = h/2m \approx 2.0 \times 10^{-3}\,\mathrm{cm}^2\,\mathrm{s}^{-1}$ and has a size

$$\xi_\mathrm{v} \approx 1.5{\times}10^{-12}\,(1 - x_\mathrm{p})^{1/3} \left(\frac{m}{m_\mathrm{n}^*}\right) \rho_{14}^{1/3} \left(\frac{10^{10}\,\mathrm{K}}{T_\mathrm{cn}}\right) \mathrm{cm}. \qquad (2)$$

Background

Quantised vorticity

- The vortices arrange themselves in a **hexagonal array** (Abrikosov, 1957) and their circulation mimics solid-body rotation on large scales. The **averaged vorticity** and **vortex area density** are given by

$$\boldsymbol{\omega} = 2\boldsymbol{\Omega} = \mathcal{N}_{\rm v}\kappa\hat{\boldsymbol{z}}, \qquad \mathcal{N}_{\rm v} \approx 6.3\times10^{5}\left(\frac{10\,{\rm ms}}{P}\right){\rm cm}^{-2}. \qquad (3)$$

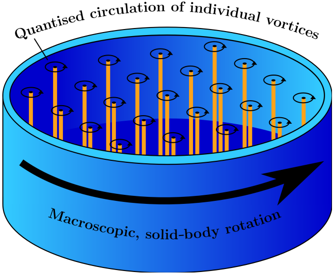

Figure 2: Vortex array of a rotating superfluid mimics solid-body rotation.

- For a regular array, the **intervortex distance** is given by $d_{\rm v} \simeq \mathcal{N}_{\rm v}^{-1/2}$:

$$d_{\rm v} \approx 1.3\times10^{-3}\left(\frac{P}{10\,{\rm ms}}\right)^{1/2}{\rm cm}. \qquad (4)$$

A change in angular momentum is achieved by creating (spin-up) or destroying (spin-down) vortices.

Mutual friction

- The vortices interact with the viscous fluid component causing dissipation. This **mutual friction** influences laboratory systems (Hall and Vinen, 1956) and neutron stars (Alpar et al., 1984b).

- Taking $\boldsymbol{\Omega} = \Omega\,\hat{\boldsymbol{\Omega}}$, the **vortex-averaged** drag force in the core is

$$\boldsymbol{F}_{\rm mf} = 2\mathcal{B}\rho_{\rm n}\,\hat{\boldsymbol{\Omega}} \times [\boldsymbol{\Omega} \times (\boldsymbol{v}_{\rm n} - \boldsymbol{v}_{\rm e})] + 2\mathcal{B}'\rho_{\rm n}\,\boldsymbol{\Omega} \times (\boldsymbol{v}_{\rm n} - \boldsymbol{v}_{\rm e})\,. \qquad (5)$$

- The **dimensionless parameters** $\mathcal{B}$ and $\mathcal{B}'$ reflect the strength of $\boldsymbol{F}_{\rm mf}$. They are calculated by considering mesoscopic **coupling physics** for a single vortex and then averaging for the full array:

$$\mathcal{B} \equiv \frac{\mathcal{R}}{1+\mathcal{R}^2}, \qquad \mathcal{B}' \equiv \frac{\mathcal{R}^2}{1+\mathcal{R}^2}. \qquad (6)$$

- Different processes affect **vortex dynamics** in the crust and the core:
  - phonon excitations (Jones, 1990)
  - Kelvin wave excitations (Epstein and Baym, 1992; Jones, 1992)
  - electron quasi-particle scattering (Feibelman, 1971)
  - scattering of electrons off the vortex magnetic field (Alpar et al., 1984b; Andersson et al., 2006)
  - Kelvin wave excitations (Link, 2003)

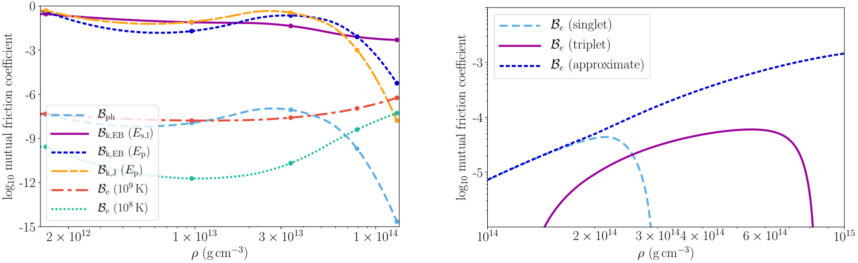

Figure 3: Mutual friction coefficients in the inner crust (left) and the core (right).

Background — Coupling mechanisms

- Different processes affect **vortex dynamics** in the crust and the core:
  - phonon excitations (Jones, 1990)
  - Kelvin wave excitations (Epstein and Baym, 1992; Jones, 1992)
  - electron quasi-particle scattering (Feibelman, 1971)
  - scattering of electrons off the vortex magnetic field (Alpar et al., 1984b; Andersson et al., 2006)
  - Kelvin wave excitations (Link, 2003)

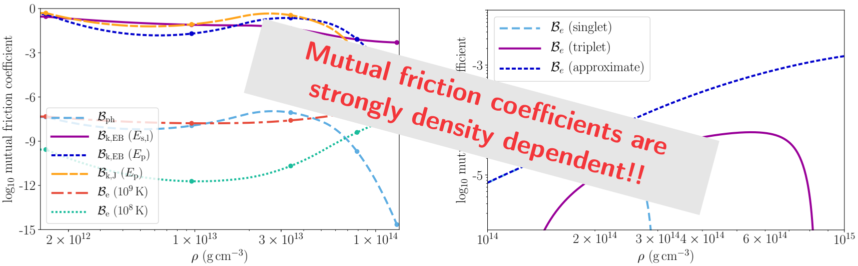

Figure 3: Mutual friction coefficients in the inner crust (left) and the core (right).

Glitches

Basics

- Glitches are sudden spin-ups caused by **angular momentum transfer** from a crustal superfluid, decoupled from the lattice (and everything tightly coupled) due to vortex pinning (Anderson and Itoh, 1975).

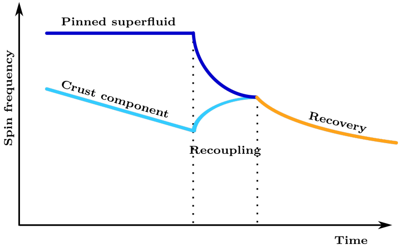

Figure 4: Sketch of an idealised glitch.

- Catastrophic vortex unpinning triggers the glitch and frictional forces acting on **free vortices** govern the **neutron star's post-glitch response**.
- Models of **long-term behaviour** have been compared to observed **exponential relaxation timescales** to analyse crustal pinning forces and temperatures (Alpar et al., 1984a, e.g.).

- Observations suggest that the **crust spin-up** after a glitch is very fast (Dodson et al., 2007; Palfreyman et al., 2018; Ashton et al., 2019 submitted).

Kelvin wave coupling

- In **hydrodynamical models**, fast recoupling is captured by Kelvin wave **mutual friction** $\Rightarrow$ study glitch rise to analyse corresponding physics.

- Reanalyse Epstein and Baym (1992) and Jones (1992) to understand discrepancies between the two and **determine drag** coefficient $\mathcal{R}$:

$$\boxed{\mathcal{R}_{\rm EB} \simeq 2.8 \left(\frac{\mu}{\hbar}\right)^{1/2} \left(\frac{E_{\rm p}\delta}{\rho_{\rm s}\kappa}\right)^{1/2} \frac{R_{\rm N}}{a^{3/2}},} \qquad \boxed{\mathcal{R}_{\rm J} \simeq \frac{1}{2\sqrt{\pi}} \left(\frac{\mu}{\hbar}\right)^{1/2} \left(\frac{E_{\rm p}\delta}{\rho_{\rm s}\kappa}\right)^{1/2} \frac{a^{1/2}}{\xi},} \tag{7}$$

with effective mass $\mu(k) \equiv -2m_{\rm u}/\ln k\xi \simeq m_u/2$ and reduction factor δ due to averaging the microscopic pinning interaction over a mesoscopic vortex length scale (Seveso et al., 2016).

Calculate $\mathcal{B}_{\rm crust} \simeq \mathcal{R}$ for realistic crust model parameters.

Density-dependence

- We use the **crustal composition** of Negele and Vautherin (1973) and pinning **interaction parameters** from Epstein and Baym (1992) and Donati and Pizzochero (2006) to calculate $\mathcal{B}_{\rm crust}$. Note that the **bottom of the crust** carries the majority of the crustal mass.

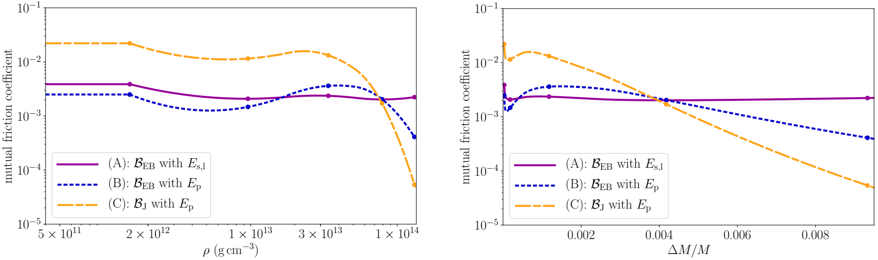

Figure 5: Mutual friction strength for kelvin wave coupling as a function of (left) density and (right) relative overlying mass fraction.

Three-component model

- **Decompose** the neutron star into crust superfluid, core superfluid and a non-superfluid 'crust' component. The latter two rotate rigidly and are coupled via a constant mutual friction coefficient $\mathcal{B}_{\rm core} \approx 5 \times 10^{-5}$.

- Neglecting entrainment for simplicity, the **equations of motion** are

$$\dot{\Omega}_{\rm sf} = \mathcal{B}_{\rm crust} \left[2\Omega_{\rm sf} + \tilde{r}\,\frac{\partial \Omega_{\rm sf}}{\partial \tilde{r}} \right] (\Omega_{\rm crust} - \Omega_{\rm sf}), \tag{8}$$

$$\dot{\Omega}_{\rm core} = \mathcal{B}_{\rm core} 2\Omega_{\rm core}\, (\Omega_{\rm crust} - \Omega_{\rm core}), \tag{9}$$

$$\dot{\Omega}_{\rm crust} = -\frac{N_{\rm ext}}{I_{\rm crust}} - \frac{I_{\rm core}}{I_{\rm crust}}\,\dot{\Omega}_{\rm core} - \frac{1}{I_{\rm crust}} \int \rho \tilde{r}^2 \dot{\Omega}_{\rm sf}\, \mathrm{d}V. \tag{10}$$

- Relate ρ and $\tilde{r}$ in the crust by solving the **TOV equations** for a realistic EoS to obtain $\mathcal{B}_{\rm crust}(\tilde{r})$ and integrate (8)-(10) in cylindrical geometry for **Vela pulsar** parameters ($\Omega_{\rm crust}(0) \approx 70\,\mathrm{Hz}$, $\Delta\Omega_{\rm crit} \approx 10^{-2}\,\mathrm{Hz}$) for $120\,\mathrm{s}$.

Differential rotation

- The superfluid rotates **differentially** due to the $\mathcal{B}_{\rm crust}(\tilde{r})$-dependence. In the outer layers, $\mathcal{B}_{\rm crust}$ is strongest and the superfluid couples first. Eventually, the superfluid has transferred all excess angular momentum and spun down to a **new steady state**, where all components corotate.

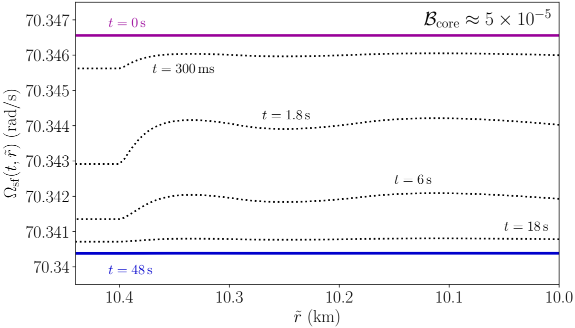

Figure 6: $\Omega_{\rm sf}$ as function of radius and time calculated for drag profile (A).

Crustal evolution

- We compare different **friction profiles** by computing the change in crust frequency $\Delta\nu$. The glitch rise shape depends crucially on the **relative strength** of the crust and core mutual friction.
- With $\mathcal{B}_{\rm core} \sim 5 \times 10^{-5}$, the crust coupling is faster than core coupling, creating a characteristic **overshoot** feature. The onset of crust-core coupling is visible as a break in the **phase shift** ϕ.

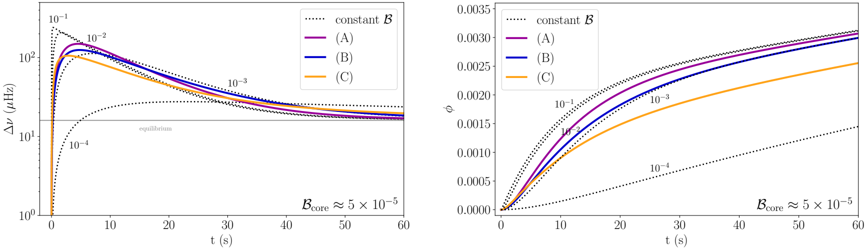

Figure 7: Change in crustal frequency $\Delta\nu(t) = [\Omega_{\rm crust}(t) - \Omega_{\rm crust}(0)]/2\pi$ and phase shift $\phi = \int \Delta\nu \, {\rm d}t$.

Observations

Preliminary comparison I

- First single-pulse observations of a glitch in the Vela pulsar (Palfreyman et al., 2018) allow a **comparison** between the data and our predictions.
- Model **timing residuals** $\Delta t \simeq -2\pi\phi/\Omega_{\mathrm{crust}}(0)$ are compared to observed residuals. We include a shift $\Delta t_0 \approx 0.22\,\mathrm{ms}$ at the time of the glitch.

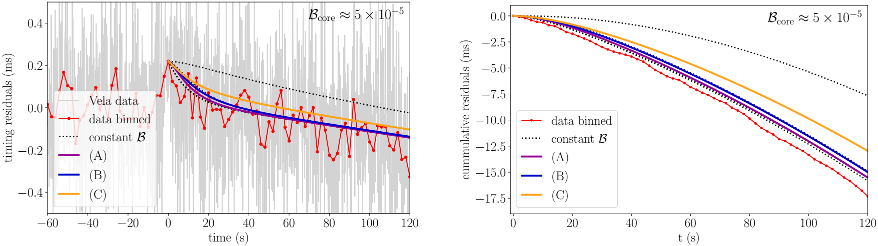

Figure 8: Comparison between theoretical (left) timing residuals and (right) cumulative residuals.

Shape is insensitive to crustal profiles as long as $\mathcal{B}_{\mathrm{crust}} \gtrsim 10^{-3}$.

- Analyse how sensitive the glitch rise is to $\mathcal{B}_{\rm core}$ for crustal profile (A):

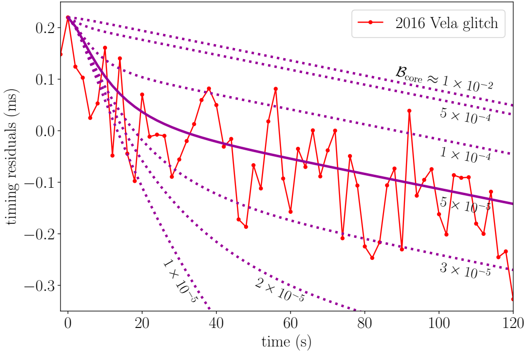

Figure 9: Comparison between the 2016 Vela glitch data and theoretical predictions calculated for drag profile (A) and a varying crust-core mutual friction strength $\mathcal{B}_{\rm core}$.

The data suggests a narrow range $3 \times 10^{-5} \lesssim \mathcal{B}_{\rm core} \lesssim 10^{-4}$.

Improved comparison I

- Use a **Bayesian framework** to fit phenomenological models of the star's rotation frequency to the Vela pulsar data (Ashton et al., 2019 submitted).
- Constrain the **glitch rise time** to less than **12.6** s with 90% confidence.

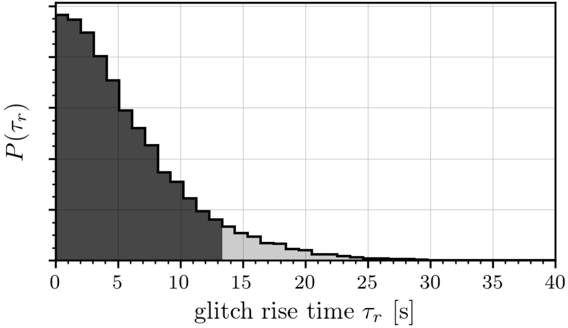

Figure 10: Posterior distribution for the rise time of the glitch. The dark shaded region marks the 90% confidence interval.

Improved comparison II

- We find definite evidence for an **overshoot** and fast decay timescale $\sim 55\,\mathrm{s} \Rightarrow$ requires three components in a body-averaged formalism.
- We find evidence for a **slow-down** of the star's rotation immediately prior to the glitch $\Rightarrow$ some **noise** process may trigger the glitch by causing a **critical lag** between crustal superfluid and the lattice.

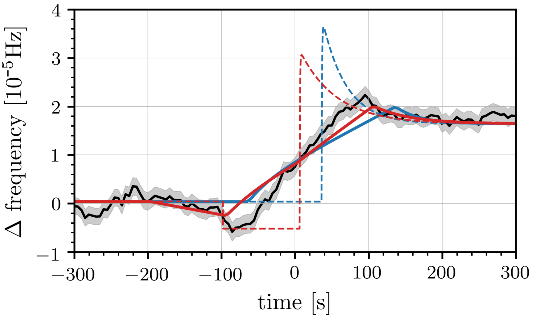

Figure 11: Frequency evolution during the 2016 Vela glitch: constant frequency model fitted with 200 s-long sliding window with 90% confidence interval (grey) plus maximum-likelihood fits for the overshoot (blue) and slow-down+overshoot (red) models. Dashed curves show the raw frequency evolution, while the solid ones show the time-averaged frequency evolution.

Conclusions

- Combine realistic crustal **Kelvin-wave profiles** with a simple treatment of the core mutual friction and implement both in a **three-component** neutron star framework $\Rightarrow$ predictive model suggests that glitch shape depends crucially on the **relative strength** between $\mathcal{B}_{\rm crust}$ and $\mathcal{B}_{\rm core}$.

- **Preliminary comparison** between our models and the first pulse-to-pulse **glitch observations** suggest strong crustal combined with weak core mutual frictional $\Rightarrow$ i.e. $\boldsymbol{\mathcal{B}_{\rm crust} \gtrsim 10^{-3}}$ and $\boldsymbol{3 \times 10^{-5} \lesssim \mathcal{B}_{\rm core} \lesssim 10^{-4}}$.

- **Bayesian framework** allows us to compare phenomenological models and deduce constraints in a model-agnostic way $\Rightarrow$ constrain the **rise time** to $< \mathbf{12.6}\,\mathrm{s}$, find evidence for overshoot and pre-glitch slow-down.

How does entrainment / the pasta phase entrainment play into this?

Thank you.

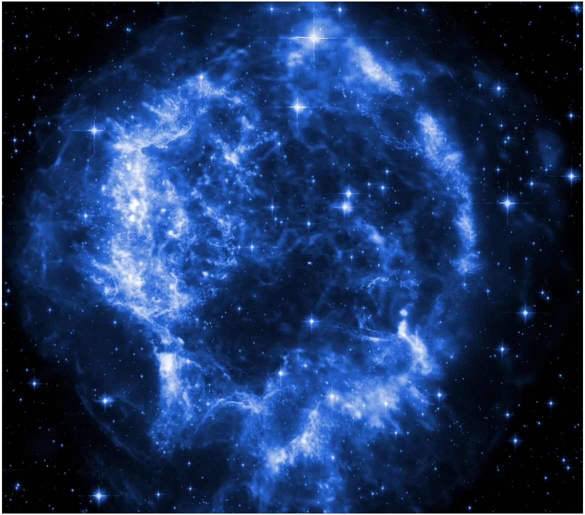

Appendix

Kelvin waves

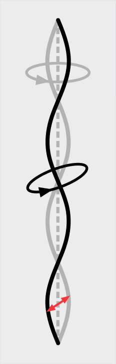

- In the absence of forces, a vortex supports **Kelvin waves** with angular frequency $\omega_k = Tk^2/\rho_s\kappa = \hbar k^2/2\mu(k)$ (Thomson, 1880), with tension T and effective mass $\mu(k) \simeq -2m_u/\ln k\xi$.

- Vortex-nucleus **interactions** excite waves with wave numbers $k \lesssim k_* \equiv (2\mu\Delta v/\hbar l)^{1/2} \Rightarrow$ determine the power p transferred into Kelvin waves and relate it to the **resistive force**, $f_{res} = p/\Delta v$.

- Epstein & Baym and Jones make **different assumptions** about p and the interaction potential including the typical interaction scale ℓ:

$$E_{EB}(s) = \frac{E_s}{(1+s^2/R_N^2)^4} + \frac{E_l}{1+s^2/R_N^2}, \qquad E_J(s) = E_p \exp\left(-\frac{s^2}{2\xi^2}\right), \quad (11)$$

where s is the separation, E_s (E_l) a short-range (long-range) interaction contribution, R_N the nuclear radius and ξ the coherence length.

Drag coefficients

- Drag coefficients depend on the relative **vortex-nucleus velocity**, but E_p and Δv are connected by a mesoscopic force balance, $\Delta v \simeq f_\mathrm{pin}/\rho_\mathrm{s}\kappa \sim E_\mathrm{p}/la\rho_\mathrm{s}\kappa$, for a pinning force f_pin per unit length and lattice spacing a.

- Correcting several errors in Epstein and Baym (1992) and accounting for a **reduction factor** δ due to averaging the microscopic pinning interaction over a mesoscopic vortex length scale (Seveso et al., 2016), we find

$$\boxed{\mathcal{R}_\mathrm{EB} \simeq 2.8 \left(\frac{\mu}{\hbar}\right)^{1/2} \left(\frac{E_\mathrm{p}\delta}{\rho_\mathrm{s}\kappa}\right)^{1/2} \frac{R_\mathrm{N}}{a^{3/2}},} \qquad \boxed{\mathcal{R}_\mathrm{J} \simeq \frac{1}{2\sqrt{\pi}} \left(\frac{\mu}{\hbar}\right)^{1/2} \left(\frac{E_\mathrm{p}\delta}{\rho_\mathrm{s}\kappa}\right)^{1/2} \frac{a^{1/2}}{\xi},} \tag{12}$$

with $E_\mathrm{p}^2 \simeq E_\mathrm{s}^2 + E_\mathrm{l}E_\mathrm{s} + 0.5E_\mathrm{l}^2$ in Epstein and Baym's formalism.

Appendix

Microscopic input

Table 1: Equilibrium composition for five crustal regions taken from Negele and Vautherin (1973) plus vortex-nucleus interaction parameters from Epstein and Baym (1992) and Donati and Pizzochero (2006).

	I	II	III	IV	V
n_{b} $[10^{-4}\,\mathrm{fm}^{-3}]$	8.8	57.7	204.0	475.0	789.0
Z	40	50	50	40	32
N	280	1050	1750	1460	950
$\tilde{x}$	0.53	0.45	0.35	0.28	0.16
n_{s} $[10^{-4}\,\mathrm{fm}^{-3}]$	4.8	47.0	184.0	436.0	737.0
ρ $[10^{12}\,\mathrm{g\,cm}^{-3}]$	1.5	9.6	33.9	78.9	131.0
A	115	161	193	183	232
R_{WS} [fm]	44.3	35.7	27.6	19.6	14.4
n_{l} $[10^{-6}\,\mathrm{fm}^{-3}]$	2.7	5.2	11.3	31.7	80.3
a [fm]	90.0	72.5	56.1	39.8	29.2
R_{N} [fm]	5.9	6.7	7.2	7.3	7.2
E_{s} [MeV]	0.42	−0.13	−1.64	−1.00	−0.78
E_{l} [MeV]	0.16	0.94	1.40	1.00	0.49
Δ [MeV]	0.21	0.68	0.91	0.56	0.19
ξ [fm]	15.6	10.1	12.0	26.1	90.8
E_{p} [MeV]	0.21	0.29	−2.74	−0.72	−0.02

- With $\mathcal{B}_{\text{core}} \sim 10^{-2}$ (due to Kelvin wave dissipation), the crustal coupling is slower than core coupling, causing the glitch rise to be **monotonic in time**. The onset of crust-core coupling is not visible in the **phase shift** ϕ.

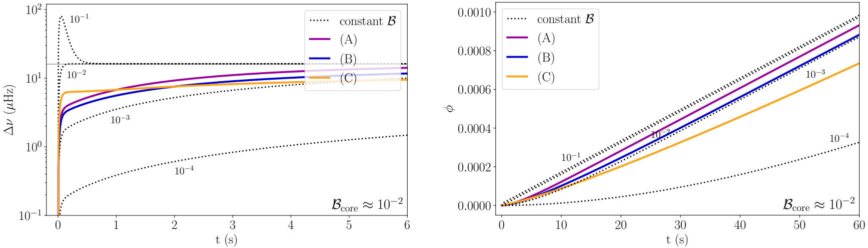

Figure 12: Change in crustal frequency $\Delta\nu(t) = [\Omega_{\text{crust}}(t) - \Omega_{\text{crust}}(0)]/2\pi$ and phase shift $\phi = \int \Delta\nu \, \mathrm{d}t$.

References I

Abrikosov, A. A. (1957). The magnetic properties of superconducting alloys. *JPCS*, 2(3):199–208.

Alpar, M. A., Anderson, P. W., Pines, D., and Shaham, J. (1984a). Vortex creep and the internal temperature of neutron stars. II - VELA pulsar. *ApJ*, 278:791–805.

Alpar, M. A., Langer, S. A., and Sauls, J. A. (1984b). Rapid postglitch spin-up of the superfluid core in pulsars. *ApJ*, 282:533–541.

Anderson, P. W. and Itoh, N. (1975). Pulsar glitches and restlessness as a hard superfluidity phenomenon. *Natur*, 256(5512):25–27.

Andersson, N., Sidery, T., and Comer, G. L. (2006). Mutual friction in superfluid neutron stars. *MNRAS*, 368(1):162–170.

Ashton, G., Lasky, P. D., Graber, V., and Palfreyman, J. L. (2019). Internal neutron-star physics from the 2016 Vela glitch. *submitted*.

Dodson, R., Lewis, D., and McCulloch, P. (2007). Two decades of pulsar timing of Vela. *Ap&SS*, 308(1-4):585–589.

Donati, P. and Pizzochero, P. M. (2006). Realistic energies for vortex pinning in intermediate-density neutron star matter. *PhLB*, 640(3):74–81.

Epstein, R. I. and Baym, G. (1992). Vortex drag and the spin-up time scale for pulsar glitches. *ApJ*, 387:276–287.

Feibelman, P. J. (1971). Relaxation of Electron Velocity in a Rotating Neutron Superfluid: Application to the Relaxation of a Pulsar's Slowdown Rate. *PhRvD*, 4(6):1589–1597.

Hall, H. E. and Vinen, W. F. (1956). The Rotation of Liquid Helium II. II. The Theory of Mutual Friction in Uniformly Rotating Helium II. *PSPSA*, 238(1213):215–234.

Jones, P. B. (1990). Rotation of the neutron-drip superfluid in pulsars: The resistive force. *MNRAS*, 243:257–262.

References II

Jones, P. B. (1992). Rotation of the neutron-drip superfluid in pulsars: The Kelvin phonon contribution to dissipation. *MNRAS*, 257(3):501–506.

Link, B. (2003). Constraining Hadronic Superfluidity with Neutron Star Precession. *PhRvL*, 91(10):101101.

Negele, J. W. and Vautherin, D. (1973). Neutron star matter at sub-nuclear densities. *NuPhA*, 207(2):298–320.

Palfreyman, J., Dickey, J. M., Hotan, A., Ellingsen, S., and van Straten, W. (2018). Alteration of the magnetosphere of the Vela pulsar during a glitch. *Natur*, 556(7700):219–222.

Seveso, S., Pizzochero, P. M., Grill, F., and Haskell, B. (2016). Mesoscopic pinning forces in neutron star crusts. *MNRAS*, 455(4):3952–3967.

Thomson, W. (1880). Vibrations of a columnar vortex. *PMag*, 10(61):155–168.